We used the QSPR model for predicting the chlorine demand in drinking water (Luilo and Cabaniss, 2010) to estimate the chlorine demand of the amino acids and amino sugars studied. The results showed that all compounds, with the exception of arginine and glutamine were predicted within ± 2.48 standard deviations of prediction, for 2% error margins for both sides (Fig. 3).

The standard deviation of prediction is ± 2SDE, and in this case the SDE for QSPR calibration at 95% confidence interval was 1.24 mol-Cl_2/mol-Cp. Any predicted data

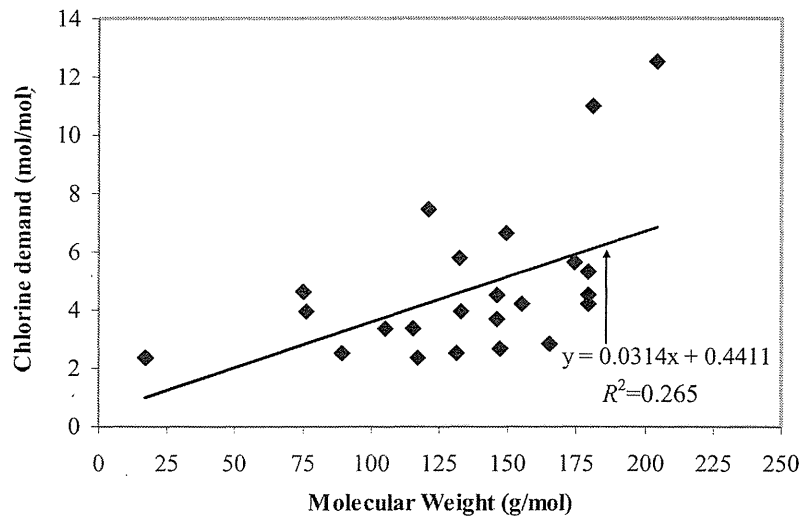

Fig. 2 - Weak correlation between chlorine demands and molecular weights of the 23 model compounds.

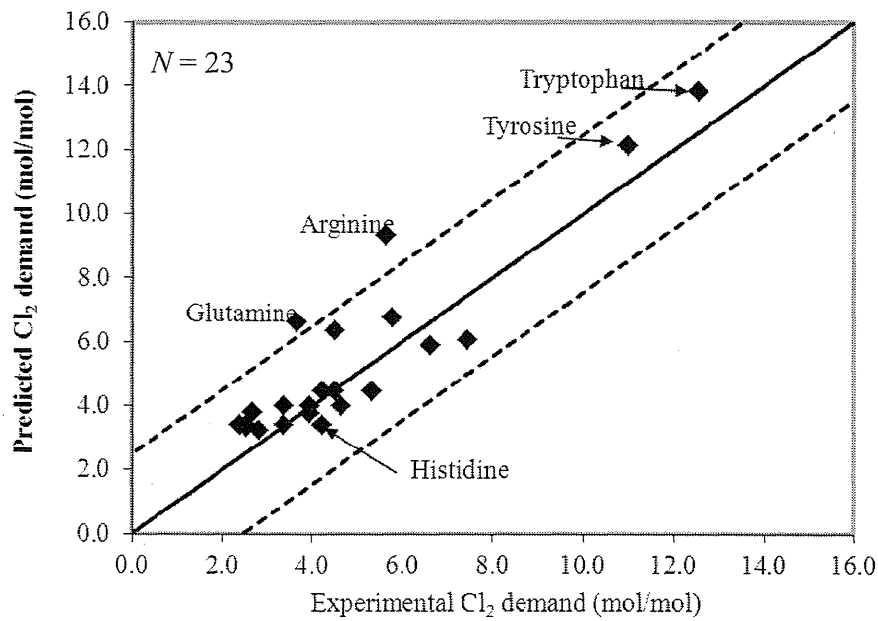

Fig. 3 - Relationship between predicted and experimental chlorine demands for the 23 amino acids. The solid line is for the ideal model and dotted lines are standard deviation of prediction margins (± 2.48 mol-Cl_2/mol-Cp).

point outside ± 2.48 margins implies that its prediction by the QSPR has some uncertainty and therefore, the predicted value may not be reliable.

To determine the reliability of the prediction, we used the coefficient of determination for cross-validation, q^2, as described previously (Luilo and Cabaniss, 2010). The value of q^2 was 0.74 which is much higher than the cut off value of 0.5 (Golbraikh and Tropsha, 2002) and RMSE equal to 1.30 mol-Cl_2/mol-Cp is closer to the model's standard error of 1.24 mol-Cl_2/mol-Cp. However, the MBD of 11.9% indicates that the model predicted 15 out of 24 compounds, which is slightly higher than expected. Although chlorine demand prediction data for tryptophan and histidine were close to the observed data, the chlorine demand prediction for histidine may not be as reliable as that for tryptophan. This is because the QSPR calibration data did not include any molecules with endocylic heteroatoms such as nitrogen (e.g., imidazole, indole, pyrrole). Thus, one limitation of QSPR is that it cannot give reliable prediction of chlorine demands of aromatic molecules without exocylic ring activators such as histidine because RAI descriptor is zero. However, RAI may be calculated in tryptophan because the amine group, which is exocyclic to the benzene ring (pyrrolyl moeity) may induce electrophilic susbstitution reaction in the benzene ring through resonance. However, the model cannot estimate the contribution of chlorine demand from the chlorine substitution at the pyrrolyl ring which has the endocyclic amine group.

The predictive power of the QSPR on model compounds is tested by generating regression line in a plot of predicted chlorine demand against the observed chlorine demand with and without intercept (Fig. 4). A good prediction should not give significantly different slopes that are closer to 1 ($0.85 \leq k \leq 1.15$); y-intercept, b, should

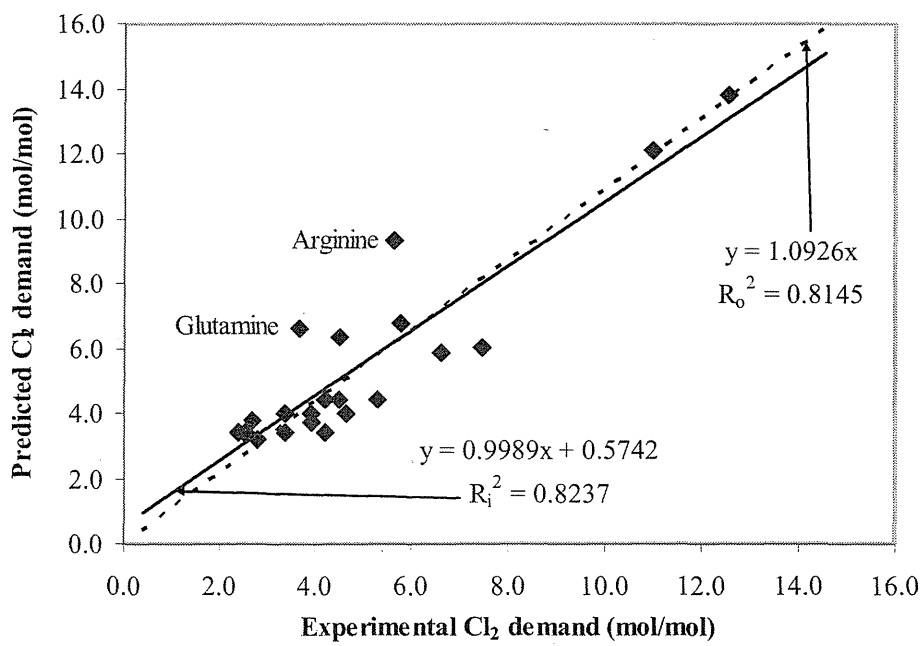

Fig. 4 - Normal regression of predicted chlorine demand against the experimental chlorine demand with y-intercept (solid line) and without y-intercept (dotted line) for 23 model compounds.

be closer to zero (b ≈ 0); and the ratio $(R_i^2 - R_o^2)/R_i^2 < 0.1$ (Golbraikh and Tropsha, 2002; Tropsha *et al.*, 2003) where R_i^2 is obtained using regression line with intercept and R_o^2 is obtained from regression line through origin. In Fig. 4, k_i is 0.998; k_o is 1.092; R_i^2 is 0.82; R_o^2 is 0.81 and the ratio $(R_i^2 - R_o^2) / R_i^2$ is 0.01, which imply that the predictive strength of the model is high.

It is interesting that arginine has three amines and one imine. Despite having the greatest number of reduced nitrogens (amine and imine) in the molecule, its chorine demand (5.63 mol-Cl_2/mol-Cp) was comparable to those of asparagine (2 amine groups) and amino sugars (1 amine group). It is possible that if the contact time used in the present study was extended to 72 h or more, arginine would have consumed more chlorine. This is because chlorination of arginine for 72 h and 96 h indicated chlorine demands of 8.20 and 8.90 mol-Cl_2/mol-Cp, respectively (Hureiki *et al.*, 1994; Hong *et al.*, 2009), which are close to the predicted value of 9.34 mol-Cl_2/mol-Cp. These observations imply that arginine reacts slowly with chlorine and therefore, requires a longer contact time for depletion. Thus, arginine is likely to continue reacting with residual chlorine in the distribution system.

CONCLUSIONS AND RECOMMENDATIONS

Amino acids and amino sugars are included among the dissolved organic matter that must be removed from raw water. However, conventional water treatment processes cannot remove all fractions of nitrogenous compounds, and are therefore likely to contribute to the chlorine demand of water. This study showed that the aromatic amino acids consumed 10 - 13 mol-Cl_2/mol-Cp, whereas the chlorine consumption of S-amino acids was between 6 and 8 mol-Cl_2/mol-Cp. The remaining amino acids and the three amino sugars showed chlorine consumption ranging between 2 and 6 mol-Cl_2/mol-Cp. The findings of our 24-h study were compared to those of the previous studies with contact times of 72 h and 96 h, and the results indicated an increasing trend in chlorine demands with time for some of the nitrogenous compounds. The QSPR predictions showed that arginine was overpredicted, while the rest were within the model prediction error.

The results of the present study indicated that chlorine demand in 24 h showed a good correlation with prediction data. Furthermore, kinetic studies are required to determine how fast the precursors can react with chlorine at typical water treatment contact times and chlorine doses. The data will provide insight into the amounts of chlorine demand and production of disinfection byproducts, especially nitrogenous compounds related to odor, while the results of longer contact times, such as 72 h and 96 h, might be useful to drive the reaction to completion.

ACKNOWLEDGMENTS

The authors would like to express their sincere gratitude to Mr. Takafumi Ito (Department of Waterworks, Kushiro, Japan) and Ms. Kyoko Suzuki (Yokohama Waterworks Bureau, Yokohama, Japan) for their experimental support. This work was partly supported by a Grant-in-aid for Health, Labor, and Welfare Research.

REFERENCES

ACC (American Chemical Council) (2008) The Benefits of Chlorine Chemistry in Water Treatment. Report prepared by Whitfield & Associates for the Chlorine Chemistry Division of the American Chemistry Council, Washington, USA.

Andersson Y. and Bohan P. (2001) Disease surveillance and waterborne disease outbreaks. In: *Water Quality Guidelines, Standards and Health*, Eds. Fewtrell L. and Bartram J., Chapter 6, pp.115-133, WHO & IWA Publishers, London, UK.

Arnold W. A., Bolotin J., von Gunten U. and Hofstetter T. B. (2008) Evaluation of functional groups responsible for chloroform formation during water chlorination using compound specific isotope analysis. *Environ. Sci. Technol.*, **42**, 7778-7785.

Ballester F. and Sunyer J. (2000) Water and health: precaution must be guided for the health of the public. *J. Epidemiol. Community Health*, **54**, 729-730.

Brosillon S., Lemasle M., Renault E., Tozza D., Heim V. and Laplanche A. (2009) Analysis and occurrence of odorous disinfection by-products from chlorination of amino acids in three different drinking water treatment plants and corresponding distribution networks. *Chemosphere*, **77**(8), 1035-1042.

Bull R. J., Reckhow D. A., Rotello V., Bull O. M. and Kim J. (2006) Use of toxicological and chemical models to prioritize DBP research. AWWA Research Foundation, Colorado, USA.

Chaidou C. I., Georgakilas V. I., Stalikas C., Saraçi M. and Lahaniatis E. S. (1999) Formation of chloroform by aqueous chlorination of organic compounds. *Chemosphere*, **39**(4), 587-594.

Chu W-H., Gao N-Y., Deng Y. and Dong B-Z. (2009) Formation of chloroform during chlorination of alanine in drinking water. *Chemosphere*, **77**(10), 1346-1351.

Clesceri L. S., Greenberg A. E. and Eaton A. D. (eds) (1998) Standard methods for the examination of water and wastewater. 20th edition, American Public Health Association, Washington DC, USA.

Crittenden J. C., Trussell R. R., Hand D. W., Howe K. J. and Tchobanoglous G. (2005) Water treatment: Principles and design, 2nd edition. John Wiley & Sons Inc., New York, USA.

de Laat J., Merlet N. and Doré M. (1982) Chlorination of organic compounds: chlorine demand and reactivity in relationship to the trihalomethane formation. *Water Res.*, **16**, 1437-1441.

Dotson, A. and Westerhoff, P. (2009) Occurrence and removal of amino acids during drinking water treatment. *J. Am. Water Works Assoc.*, **101**(9), 101-115.

Eaton A. D., Clesceri L. S., Rice E. W., Greenberg A. E. and Franson M. A. H. (eds) (2005) Standard methods for the examination of water and wastewater. 21st edition, American Public Health Association, Washington DC, USA.

Galal-Gorchev H. (1996) Chlorine in water disinfection. *Pure Appl. Chem.*, **68**(9), 1731-1735.

Gallard H. and von Gunten U. (2002) Chlorination of phenols: Kinetics and formation of chloroform. *Environ. Sci. Technol.*, **36**, 884-890.

Golbraikh A. and Tropsha A. (2002) Beware of q^2. *J. Mol. Graphics Model*, **20**(4), 269-276.

Griffith D. C., Kelly-Hope L. A. and Miller M. A. (2006) Review of reported cholera outbreaks worldwide. *Am. J. Trop. Med. Hyg.*, **75**(5), 973-977.

Hermer R. (1999) Water quality and health. *The Environmentalist*, **19**(1), 11-16.

Hong H. C., Wong M. H. and Liang Y. (2009) Amino acids as precursors of

trihalomethane and haloacetic acid formation during chlorination. *Arch. Environ. Toxicol.*, **56**, 638-645.

Hureiki L., Croué J. P. and Legube B. (1994) Chlorination studies of free and combined amino acids. *Water Res.*, **28**, 2521-2531.

Hutin Y., Luby S. and Paquet C. (2003) A large cholera outbreak in Kano City, Nigeria: the importance of hand washing with soap and the danger of street-vended water. *J. Water Health*, **1**(1), 45-52.

Larson R. A. and Weber E. J. (1994) Reaction mechanisms in environmental organic chemistry. Lewis Publishers, New York, USA.

Lee S. H., Levy D. A., Craun G. F., Beach M. J. and Calderon R. L. (2002) Surveillance for waterborne-disease outbreaks-United States 1999-2000. *Morb. Mortal. Wkly Rep.*, **51**(SS-8), 1-147.

Luilo G. B. and Cabaniss S. E. (2010) Quantitative structure-property relationship for predicting chlorine demand by organic molecules. *Environ. Sci. Technol.*, **44**(7), 2503-2508.

NRC (National Research Council) (1987) Drinking water and health, volume 7. Disinfectants and disinfection byproducts. National Academic Press, Washington DC, USA.

Peuravuori J. and Pihlaja K. (2007) Characterization of freshwater humic matter. In: *Handbook of water analysis, 2nd edition*, Ed. Nollet, L. M. L., pp435-447, CRC Press, Boca Raton, FL, USA.

Pietsch J., Sacher F., Schmidt W. and Brauch H. J. (2001) Polar nitrogen compounds and their behaviour in the drinking water treatment process. *Water Res.*, **15**(15), 3537-3544.

PNL (Pacific Northwest Laboratories) (1998) Disinfection technologies for potable water and waste water treatment: Alternatives to chlorine gas (http://www.bvsde.paho.org/bvsacd/cd25/chlorine.pdf) (accessed May, 2012).

Ribas F., Frias J. and Lucena F. (1991) A new dynamic method for the rapid determination of the biodegradable dissolved organic carbon in drinking water. *J. Appl. Bacteriol.*, **71**(4), 371-370.

Swerdlow D. L., Malenga G., Begkoyian G., Nyangulu D., Toole M., Waldman R. J., Puhr D. N. and Tauxe R. V. (1997) Epidemic cholera among refugees in Malawi, Africa: treatment and transmission. *Epidemiol. Infect.*, **118**(3), 207-214.

Tropsha A., Gramtica P. and Gomba V. K. (2003) The Importance of being earnest: Validation is absolute essential for successful application and interpretation of QSPR model. *QSAR Comb. Sci.*, **23**(1), 69-77.

USEPA (U.S. Environmental Protection Agency) (1999) *Alternative disinfectants and oxidants guidance manual*, United States Office of Water. EPA 815-R-99-014.

Volk C., Kaplan L. A., Robinson J., Johnson B., Wood L., Zhu H. W. and LeChevallier, M. (2005) Fluctuations of dissolved organic matter in river used for drinking water and impacts on conventional treatment plant performance. *Environ. Sci. Technol.*, **39**(11), 4258-4264.

Volk C., Wood L., Johnson B., Robinson J., Zhu H. W., Kaplan L. (2002) Monitoring dissolved organic carbon in surface and drinking waters. *J. Environ. Monit.*, **4**(1), 43-47.

WHO (Word Health Organization) (1998) Cholera in 1997. *Wkly Epidemiol. Rec.*, **73**, 201-208.

WQHC (Water Quality and Health Council) (2002). *Drinking Water & Health Quarterly*, **8**(1).

WATER RESEARCH 46 (2012) 4741–4749

Available online at www.sciencedirect.com

SciVerse ScienceDirect

journal homepage: www.elsevier.com/locate/watres

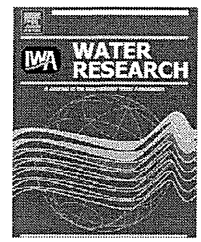

Characteristics of competitive adsorption between 2-methylisoborneol and natural organic matter on superfine and conventionally sized powdered activated carbons

Yoshihiko Matsui [a,*], *Tomoaki Yoshida* [b], *Soichi Nakao* [b], *Detlef R.U. Knappe* [c], *Taku Matsushita* [a]

[a] *Faculty of Engineering, Hokkaido University, N13W8, Sapporo 060-8628, Japan*
[b] *Graduate School of Engineering, Hokkaido University, N13W8, Sapporo 060-8628, Japan*
[c] *Department of Civil, Construction, and Environmental Engineering, North Carolina State University, Raleigh, NC 27695-7908, USA*

ARTICLE INFO

Article history:
Received 1 February 2012
Received in revised form
14 May 2012
Accepted 6 June 2012
Available online 16 June 2012

Keywords:
PAC
Particle size
Sub-micrometer
Competitive adsorption
Humic substance
Taste and odor

ABSTRACT

When treating water with activated carbon, natural organic matter (NOM) is not only a target for adsorptive removal but also an inhibitory substance that reduces the removal efficiency of trace compounds, such as 2-methylisoborneol (MIB), through adsorption competition. Recently, superfine (submicron-sized) activated carbon (SPAC) was developed by wet-milling commercially available powdered activated carbon (PAC) to a smaller particle size. It was reported that SPAC has a larger NOM adsorption capacity than PAC because NOM mainly adsorbs close to the external adsorbent particle surface (shell adsorption mechanism). Thus, SPAC with its larger specific external surface area can adsorb more NOM than PAC. The effect of higher NOM uptake on the adsorptive removal of MIB has, however, not been investigated. Results of this study show that adsorption competition between NOM and MIB did not increase when NOM uptake increased due to carbon size reduction; i.e., the increased NOM uptake by SPAC did not result in a decrease in MIB adsorption capacity beyond that obtained as a result of NOM adsorption by PAC. A simple estimation method for determining the adsorbed amount of competing NOM (NOM that reduces MIB adsorption) is presented based on the simplified equivalent background compound (EBC) method. Furthermore, the mechanism of adsorption competition is discussed based on results obtained with the simplified EBC method and the shell adsorption mechanism. Competing NOM, which likely comprises a small portion of NOM, adsorbs in internal pores of activated carbon particles as MIB does, thereby reducing the MIB adsorption capacity to a similar extent regardless of adsorbent particle size. SPAC application can be advantageous because enhanced NOM removal does not translate into less effective removal of MIB. Molecular size distribution data of NOM suggest that the competing NOM has a molecular weight similar to that of the target compound.

* *Corresponding author.* Tel./fax: +81 11 706 7280.
E-mail address: matsui@eng.hokudai.ac.jp (Y. Matsui).
0043-1354/$ – see front matter © 2012 Elsevier Ltd. All rights reserved.
http://dx.doi.org/10.1016/j.watres.2012.06.002

1. Introduction

2-methylisoborneol (MIB) is an earthy-musty odor compound that causes frequent customer complaints because it deteriorates the organoleptic qualities of drinking water. A widely accepted means for removing MIB is the addition of powdered activated carbon (PAC) prior to solid–liquid separation. MIB is a hydrophobic compound (log K_{ow} = 3.31) with small molecular size (molecular weight = 168) and is therefore efficiently adsorbed on activated carbon if it is present as a single compound in pure water. However, MIB always coexists with natural organic matter (NOM) in drinking water sources. Because NOM also adsorbs on activated carbon, it reduces the MIB adsorption capacity by competing for adsorption sites (direct site competition) and/or by hindering diffusion of MIB into carbon pores (pore blockage/constriction). NOM is also targeted for removal by many utilities because it is a precursor material for disinfection byproducts. Therefore, activated carbons that are effective for the simultaneous removal of MIB and NOM are desirable.

NOM can dramatically reduce the adsorption capacity of a micropollutant, but a micropollutant does not affect the adsorption of NOM because the concentration of NOM (mg/L) is several orders of magnitude higher than the concentration of most micropollutants including odor compounds (MIB), pesticides, and PPCPs (pharmaceuticals and personal care products), which occur at ng/L to μg/L levels. The competitive effect, namely the magnitude of the decrease in micropollutant adsorption capacity, is dependent on the loading of NOM on the carbon (Kilduff et al., 1998; Kilduff and Karanfil, 2002). Direct competition is the dominant mechanism at low NOM loading while pore blockage/constriction becomes important at high NOM loading (Kilduff et al., 1998; Matsui et al., 2003; Ding et al., 2006). It was shown that NOM of low molecular weight (MW) exerts a strong competitive effect on micropollutant adsorption (Newcombe et al., 1997, 2002b; Hepplewhite et al., 2004; Kilduff et al., 1998; Matsui et al., 2002). Low MW NOM is adsorbed to a greater extent than higher MW NOM (Matsui et al., 1993, 1998; Kilduff et al., 1996; Newcombe et al., 2002a). The resulting higher loading of low MW NOM likely exerts a greater competitive effect on micropollutant adsorption. However, even at the same loading, low MW NOM reduces micropollutant adsorption to a greater degree than high MW NOM (Kilduff et al., 1998; Matsui et al., 2002), most likely because low MW NOM can access the same adsorption sites on which micropollutants adsorb.

Although adsorption competition mechanisms between NOM and micropollutants are complex, simple quantitative modeling approaches based on multi-component adsorption theory (i.e., ideal adsorption solution theory) have been proposed and verified. One approach describing the adsorption of a micropollutant from water containing NOM utilizes an equivalent background compound (EBC) to approximate NOM (Najm et al., 1991) whereas another employs fictive components (Frick and Sontheimer, 1983; Crittenden et al., 1985). Based on the EBC approach, a simple relationship was found and validated: the percentage of micropollutant removal that can be achieved with a given carbon dose in a batch adsorption system is independent of the initial concentration of the micropollutant (Knappe et al., 1998; Gillogly et al., 1998; Graham et al., 2000). This relationship holds when the micropollutant concentration is low compared to the NOM concentration. In addition, the relationship is valid at non-equilibrium conditions in both PAC and GAC adsorption processes (Matsui et al., 2001, 2002, 2003; Zoschke et al., 2011).

To help water treatment professionals choose effective activated carbons, many studies have been conducted to better understand the mechanism of competition and to mathematically model the competitive adsorption process. However, the increased knowledge seldom results in the production of activated carbons that minimize the carbon usage rate. Some studies report enhancing the effectiveness of activated carbon for MIB removal. In one such study, PACs were tailored by changing activation conditions such that the PAC obtained with the optimized activation protocol outperformed commercially available PAC (Tennant and Mazyck, 2003). Tailoring efforts were also conducted for virgin and spent granular activated carbons to enhance their effectiveness for MIB removal (Nowack et al., 2004; Mackenzie et al., 2005). On the other hand, our research group proposed the use of superfine activated carbon (SPAC) with a particle size finer than that of traditional PAC, from which SPAC is produced by wet-milling. The design concept of SPAC was originally to improve the adsorbate uptake rate. In fact, SPAC is far superior to PAC in removing geosmin and NOM, especially at short contact times (Matsui et al., 2005, 2007, 2009). It was also found that SPAC has a higher NOM adsorption capacity than the parent PAC (Matsui et al., 2004; Ando et al., 2010). The higher NOM adsorption capacity of SPAC can be explained by the shell adsorption mechanism (SAM), which postulates that NOM molecules do not completely penetrate the adsorbent particle. Instead, they preferentially adsorb near the exterior particle surface (Ando et al., 2010, 2011; Matsui et al., 2011). As a result, a larger fraction of adsorption sites is accessible to NOM on SPAC compared to PAC due to the higher external surface area of the former. In the presence of NOM, geosmin and MIB adsorption capacities of SPAC did not become smaller than those of PAC even though NOM adsorbed to a greater extent on SPAC than on PAC (Matsui et al., 2010). This result suggests that the adsorption competition is less severe for SPAC than for PAC. However, the competitive mechanism was not inferred.

In this paper, adsorption equilibrium data of MIB and NOM were collected for SPAC and PAC and analyzed with the EBC and SAM models to elucidate differences in the mechanism of adsorption competition between MIB and NOM on PAC and SPAC.

2. Methods

2.1. *Activated carbon*

Commercially available PAC (wood-based thermally activated carbon, Taikou-W, Futamura Chemical Industries Co., Gifu, Japan) was obtained in 2008 and 2010 and prepared as a slurry in ultrapure water. PAC was pulverized into SPAC with a wet

bead mill (Metawater Co., Tokyo, Japan). In this paper, we refer to the as-received PAC obtained in 2008 as PAC08 and that obtained in 2010 as PAC10. The superfine carbons are referred to in a similar way as SPAC08 and SPAC10. Carbon properties are summarized in Table 1S (supplementary information) and the paper of Ando et al. (2010). In supplementary experiments we also used carbons that were pulverized such that median diameters were intermediate to those listed in Table 1S. Carbons were stored as slurries in ultrapure water at 4 °C and used after dilution and placement under vacuum. Particle size distributions of activated carbons were determined with a laser-light scattering instrument following the addition of a dispersant (0.02 mL of 18% anionic surfactant solution per 200 mL SPAC/PAC sample suspension containing between 0.001 and 0.01% carbon) and 4-min. sonification with ultrasound (LA-700, Horiba, Ltd., Kyoto, Japan).

2.2. *Water samples*

Waters containing NOM were collected from three lakes and one river in Japan (Table 2S). Samples were transported in polyethylene tanks and stored at 4 °C. Waters were filtered through a 0.2-μm pore size membrane (DISMIC-25HP; Toyo Roshi Kaisha, Ltd., Tokyo) and adjusted to a similar DOC concentration of ~1.5 mg-C/L by dilution with ultrapure water (Milli-Q Advantage, Millipore Co.) amended with salts to obtain a uniform ionic composition. Salt additions were selected such that the highest ion concentration in each of the NOM-containing waters was reached in all waters. In addition, SFA and SHA waters were prepared by dissolving Suwannee River humic and fulvic acids in ultrapure water amended with inorganic ions to simulate the ionic composition of the diluted natural waters (Table S2).

Stock solutions of MIB were prepared by dissolving pure MIB (Wako Pure Chemical Industries, Ltd., Osaka, Japan) in ultrapure water (Milli-Q Advantage, Millipore Co.). NOM-containing waters were spiked with the MIB stock solution to obtain an initial MIB concentration of ~1 μg/L (6 nmol/L). For single-solute MIB experiments, the MIB stock solution was added to organic-free water (OFW) amended with inorganic ions such that the ionic composition was similar to that of the diluted NOM-containing waters (Table 2S). All waters were filtered through a 0.2-μm pore size membrane before use. MIB concentrations were analyzed using a purge and trap concentrator coupled to a GC-MS (GCMS-QP2010 Plus; Shimadzu Corp., Kyoto, Japan; Aqua PT 5000 J, GL Sciences Inc., Tokyo, Japan).

Dissolved organic carbon (DOC) served as a parameter for quantifying bulk NOM concentrations (Model 810; Sievers Instruments, Inc., Boulder, CO, USA). Ultraviolet absorbance at 260 nm (UV_{260}) served as an indicator of chromophoric NOM (Model UV-240, Shimadzu Corp., Kyoto, Japan). MW distributions of NOM were determined using high performance size exclusion chromatography (HPSEC) [HP1100 (Agilent Technologies, Inc., CA, USA); packed column GL-P252 (Hitachi, Ltd.); eluent: 0.02 M Na_2HPO_4 + 0.02 M KH_2PO_4]. Polystyrene sulfonate (weight-average MW 1920, 5180, and 6130 Da) and salicylic acid (138 Da) were used for calibration (Zhou et al., 2000). The UV_{260} absorbance and DOC (Model 810 Turbo; GE Analytical Instruments) of the HPSEC column effluent were measured continuously.

2.3. *Batch adsorption tests*

In adsorption equilibrium tests, aliquots (150 mL) of OFW or NOM-containing water spiked with MIB (C_0 = ~1 μg/L) were transferred to 160-mL vials. A specified amount of SPAC/PAC was immediately added, the vials were manually shaken and then agitated on a mechanical shaker for one week at a constant temperature of 20 °C. In a preliminary experiment, it was confirmed that MIB adsorption equilibrium was reached in one week and that NOM adsorption equilibrium was almost reached. Control tests were also conducted by using multiple bottles that did not contain carbon to confirm that MIB and NOM concentration changes during long-term mixing were negligible. After filtering water samples through a 0.2-μm membrane filter, adsorbate (MIB and NOM) concentrations in the aqueous phase were measured. Solid-phase concentrations of each adsorbate were calculated from the mass balance.

3. Results and discussion

3.1. *MIB adsorption capacities on S-PAC and PAC*

MIB adsorption isotherm experiments were conducted in OFW and in 10 waters containing NOM. For all tested carbons, MIB adsorption capacities were smaller in NOM-containing waters than in OFW (Fig. 1S, supplementary information). In OFW, the MIB adsorption capacity of SPAC was slightly higher than that of PAC, but this difference was small (e.g., <30% at an aqueous-phase concentration of 0.6 nmol/L = 100 ng/L). In contrast, the MIB adsorption capacity in NOM-containing waters was only 10–40% of that obtained in OFW. Because OFW contained a similar ionic composition as the NOM-containing waters and the only difference between NOM-containing water and OFW was the presence/absence of NOM, the lower MIB adsorption capacity in NOM-containing waters should be due to adsorption competition by NOM. The ratio of the MIB adsorption capacity in NOM-containing water to that in OFW at an equilibrium aqueous-phase concentration of 0.6 nmol/L (= 100 ng/L, approximately the median concentration in the data, Fig. 1S) is summarized in Fig. 1 (values calculated from each Freundlich isotherm model fit). All experiments in NOM-containing waters were conducted at nearly the same initial NOM concentration, but the effect of NOM on MIB adsorption differed among the NOM-containing waters. The reduction in MIB adsorption capacity was higher for the NOM in Kasumigaura and Hakucho waters and lower for the NOM in Inba and Chibaberi waters. Furthermore, results in Fig. 1 show that the effect of NOM on the reduction in MIB adsorption capacity was similar for PAC and SPAC for 9 out of 10 experiments.

In experiments evaluating MIB adsorption in NOM-containing waters, aqueous-phase DOC concentrations were also measured. At a fixed carbon dose of 8 mg/L, which roughly yielded an equilibrium MIB concentration of 100 ng/L, DOC loadings on SPAC were 1.6–3.9 times those obtained with PAC (Figs. 2S and 3S). Similarly, DOC loadings were compared at

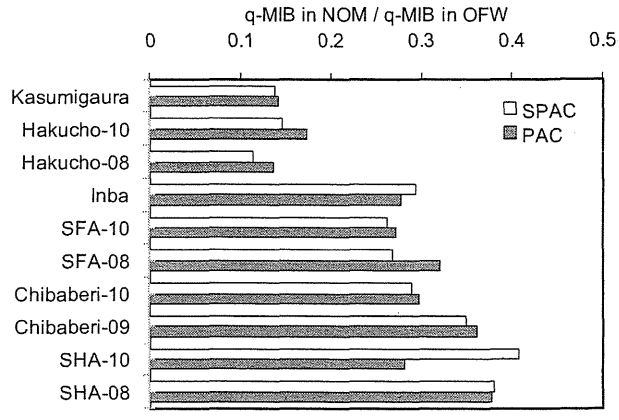

Fig. 1 – Ratio of MIB adsorption capacity in NOM-containing water to that in OFW. MIB adsorption capacities were evaluated from batch adsorption isotherm data at an equilibrium MIB aqueous-phase concentration of 0.6 nmol/L (100 ng/L).

a given equilibrium aqueous-phase MIB concentration of 100 ng/L (Fig. 2). DOC loadings were obtained from each Freundlich model fit to DOC isotherm data (q_{DOC} vs. C_{DOC}) at a carbon dose that yielded an equilibrium aqueous-phase MIB concentration of 100 ng/L. DOC loadings varied greatly among NOM sources and were consistently higher on SPAC than on PAC. DOC loadings ranged from 60 to 135 mg-C/g for SPAC and from 21 to 46 mg-C/g for PAC. In Kasumigaura water, DOC loadings were relatively low (Fig. 2), but the MIB adsorption capacity was more strongly affected than in other NOM-containing waters (Fig. 1). In contrast, Inba water yielded a higher DOC loading on both PAC and SPAC, but the effect on MIB loading was not as strong as that obtained in Kasumigaura water. Therefore, the DOC loading on the carbon is not indicative of the NOM effect on MIB adsorption capacity, and the NOM competing with MIB is likely only a fraction of the total NOM.

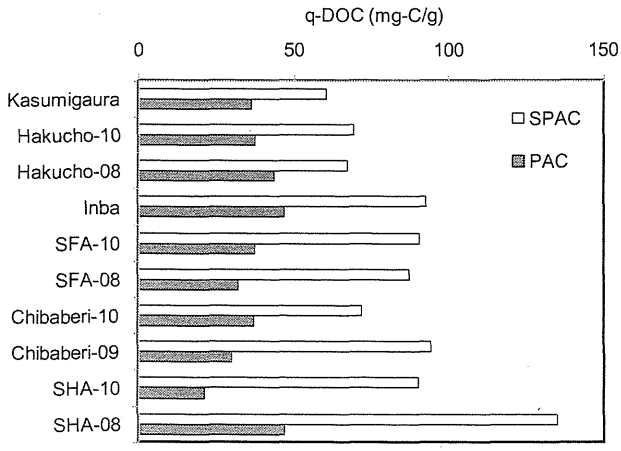

Fig. 2 – DOC loadings on each carbon at experimental conditions matching those described for Fig. 1.

3.2. *Analysis of competitive adsorption by equivalent background compound method*

To distinguish between adsorption of (1) NOM and (2) the NOM fraction that directly competes with MIB for adsorption sites, an equivalent background compound (EBC) adsorption analysis was conducted. When competing NOM is represented by a single hypothetical compound (EBC), the system containing MIB and NOM can be modeled as a bi-solute system. Incorporating the Freundlich isotherm equation into the bi-solute form of the Ideal Adsorption Solution Theory, the MIB adsorption isotherm becomes

$$C_M = \frac{q_M}{q_M + q_E}\left(\frac{n_M q_M + n_E q_E}{n_M K_M}\right)^{n_M} \quad (1)$$

where, C_M is the liquid-phase concentration of MIB (nmol/L), q_M is the solid-phase concentration of MIB (nmol/mg), q_E is the solid-phase concentration of EBC (nmol/mg), n_M and K_M are the single-solute Freundlich isotherm exponent and constant for MIB [dimensionless and (nmol/mg)/(nmol/L)$^{1/n}$, respectively], and n_E is the single-solute Freundlich isotherm exponent for the EBC (dimensionless).

With the two assumptions that (1) the EBC solid-phase concentration was much greater than the solid-phase concentration of the target compound and (2) the Freundlich exponents $1/n_M$ and $1/n_E$ are not very different, i.e., both fall into the range 0.1–1, Knappe et al. (1998) derived an equation that validated the experimentally observed direct proportionality between MIB adsorption capacity and initial MIB concentration at a given carbon dose. With the same assumptions, equation (1) becomes;

$$q_E^* = q_E n_E^{\frac{n_M}{n_M - 1}} = (n_M K_M)^{\frac{n_M}{n_M - 1}}\left(\frac{C_M}{q_M}\right)^{\frac{1}{n_M - 1}} \quad (2)$$

where, q_E^* is the pseudo solid-phase concentration for the competing NOM fraction (nmol/mg).

Equation (2) illustrates that the EBC loading (q_E) can be quantitatively estimated if C_M, q_M, n_M, K_M, and n_E are known. C_M and q_M values were obtained from MIB adsorption isotherm experiments in NOM-containing waters, and $1/n_M$ and K_M values were obtained from Freundlich model fits to MIB adsorption isotherm data obtained in OFW (Fig. 1S and Table 3S (supplementary information)). The value of $1/n_E$, Freundlich exponent of EBC, was unknown. However, the value of q_E^* defined by equation (2) can be used for comparing EBC loadings on the carbons if $1/n_E$ and $1/n_M$ values are similar among carbons. Similarity in $1/n_M$ values is demonstrated in Table 3S, and similarity in $1/n_E$ has been demonstrated in a previous study that evaluated the effects of NOM on MIB adsorption by four activated carbons (Newcombe et al., 2002b). The EBC loading (q_E) is linked to q_E^* via the term $n_E^{n_M/(n_M-1)}$, which ranges in magnitude from 3.95 to 4.67 if $1/n_E = 0.47$ (Table 1) and $1/n_M$ ranges from 0.45 to 0.51 (Table 3S). In that case, q_E is 21.4–25.3% of the q_E^* values calculated from the right hand side of equation (2).

In this study, the loading of the competing NOM fraction was estimated by calculating q_E^*. The magnitude of the pseudo-concentration decrease of the competing NOM fraction (ΔC_E^*) can be calculated from

Table 1 – Parameter values of equations (9) and (10).

Parameter	Value	
$1/n_E$	0.47	Assumed to be similar to that of MIB (the average value of n_M) (Knappe et al., 1998, Worch, 2010)
	(0.2–0.6)	Possible range
SUVA	6.1 (m^{-1} L/mg-C)	Highest observed value (Table 2S)
Carbon content	0.52 (mg-C/mg)	The value for fulvic acid (International Humic Substance Society)

$$\Delta C_E^* \equiv C_{E,0}^* - C_E^* = C_C q_E^* \quad (3)$$

where $C_E^* (= C_E n_E^{n_M/(n_M-1)})$ is the pseudo aqueous-phase concentration of the competing NOM fraction (nmol/L), $C_{E,0}^*$ is the initial pseudo aqueous-phase concentration of the competing NOM fraction (nmol/L), and C_C is the carbon dose (mg/L).

At high carbon doses, $C_E << C_{E,0}$ and $C_M << C_{M,0}$ ($C_{E,0}$ and $C_{M,0}$ are initial EBC and MIB concentrations, respectively). As a result, an isotherm for the micropollutant in natural water becomes parallel to the single-solute isotherm of the trace organic compound on a log–log scale plot between solid- and liquid-phase concentrations (Knappe, 1996; Qi et al., 2007). Therefore, the isotherm for MIB in natural water can be described by a pseudo-single solute isotherm equation with the same Freundlich exponent as that obtained for the single-solute MIB system;

$$q_M = K_M^* C_M^{\frac{1}{n_M}} \quad (4)$$

where, K_M^* is the Freundlich constant describing the MIB adsorption isotherm obtained in NOM-containing water [(nmol/mg)/(nmol/L)$^{1/n}$].

By substituting equation (4) into (2), equation (2) becomes;

$$q_E^* = q_M \left(n_M \frac{K_M}{K_M^*} \right)^{\frac{n_M}{n_M - 1}} \quad (5)$$

Therefore, once K_M and n_M are known, q_E^* values can be calculated for a given carbon dose from equation (5) after determining q_M at a given carbon dose from the mass balance (eq. (6)) and K_M^* from equation (4).

$$C_{M,0} - C_M = C_C q_M \quad (6)$$

Pseudo solid-phase concentrations of the competing NOM fraction (q_E^*) and DOC (q_{DOC}) are compared in Fig. 3. For q_E^*, values decreased with increasing carbon dose. Corresponding ΔC_E^* values increased initially with carbon dosage and plateaued at a carbon dosage of ~10 mg/L. On the other hand, ΔC_{DOC} continued to increase with increasing carbon dose even after ΔC_E^* values had plateaued. This observation suggests that the competing NOM fraction is a strongly adsorbing NOM fraction that preferentially adsorbs on carbon and is almost completely removed with relatively low carbon doses. Furthermore, values of q_E^* were similar between SPAC and PAC while values of q_{DOC} were higher on SPAC. This result directly relates to the experimental observations summarized in Figs. 1 and 2; i.e., DOC loadings are higher on SPAC than on PAC while reductions in MIB loading resulting from the presence of NOM were similar for PAC and SPAC.

Fig. 4 summarizes q_E^* values corresponding to the MIB and DOC adsorption data shown in Figs. 1 and 2 (q_E^* values at a carbon dose of 8 mg/L are shown in Fig. 4S (supplementary information)). Values of q_E^* were similar between SPAC and PAC for all tested waters, which clearly indicates that SPAC adsorbed the competing NOM fraction to a similar extent as PAC. In terms of adsorption of competing NOM, therefore, SPAC and PAC are not very different. However, SPAC adsorbed NOM to a greater extent than PAC (Fig. 2). These results mean that SPAC adsorbed non-competing NOM (NOM that is not competitive to MIB) more than PAC, but SPAC and PAC adsorbed similar amounts of competing NOM such that MIB adsorption was affected to a similar extent.

3.3. *Adsorption of competing NOM*

In Fig. 3, ΔC_E^* values plateaued once the carbon dose reached about 10 mg/L. This means that the competing NOM fraction was almost completely taken up from solution at carbon doses >10 mg/L. Therefore, the ΔC_E^* value when $C_C > 10$ mg/L should be equivalent to the concentration of the competing NOM fraction initially present in the water before dosing carbon ($C_{E,0}^*$).

Fig. 5 summarizes $C_{E,0}^*$ values for the different waters that were calculated with equations (3)–(6). $C_{E,0}^*$ values differed among the tested NOM sources (range: ~0.2 μmol/L for SHA08 to ~1.3 μmol/L for Hakucho08). However, $C_{E,0}^*$ values of a given water were almost the same between SPAC and PAC, which again shows that the competing NOM fraction is similar for SPAC and PAC.

For the waters having higher $C_{E,0}^*$ values (Hakucho and Kasumigaura waters), the difference in q_{DOC} values between SPAC and PAC was smaller than for other waters (Fig. 2). In an analogous manner, the difference in q_{DOC} values between SPAC and PAC was larger for waters with lower $C_{E,0}^*$ values (e.g., SHA and SFA waters). Ando et al. (2010, 2011) reported that the increase in DOC adsorption capacity with decreasing carbon size is due to the limited penetration distance of NOM from the exterior surface of carbon particles (shell adsorption mechanism). The specific external surface area (surface area per unit mass) available for adsorption is therefore greater for smaller adsorbent particles, and hence the DOC adsorption capacity of SPAC, which has a smaller particle size than PAC, is larger. If adsorption occurred only at the external particle surface, then the increase in DOC adsorption capacity would be inversely proportional to adsorbent particle size (i.e., the slope of log solid-phase concentration when plotted as a function of log median diameter would equal −1). In contrast, a slope of zero would indicate that DOC adsorption occurs uniformly throughout the entire carbon particle. Matsui et al. (2011) reported, however, that slope values fell between 0 and −1, indicating that a fraction of the interior region of the adsorbent particles is available for DOC adsorption. In this study, the magnitude of the inverse of the slope (i.e. gradient of log D_{50}/log q_{DOC}) is called the penetration index.

The dependence of the solid-phase DOC concentration (q_{DOC}) on median carbon diameter (D_{50}) is shown on a log–log

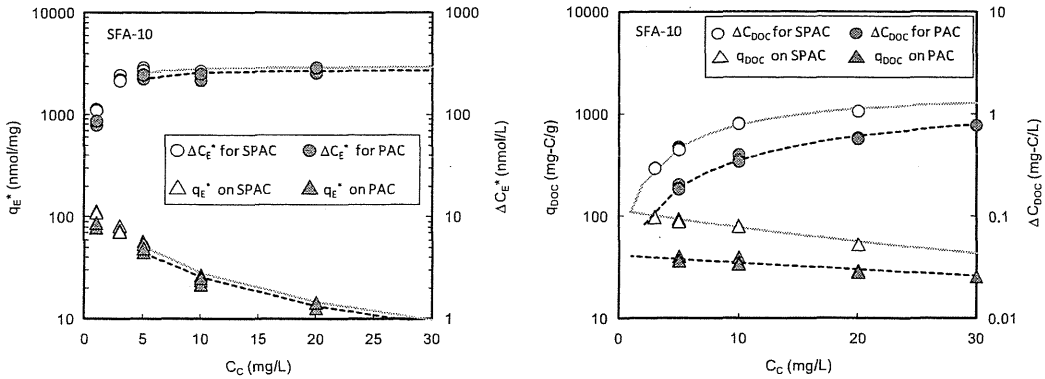

Fig. 3 – Pseudo solid-phase concentrations of the competing NOM fraction (q_E^*) and the corresponding pseudo aqueous-phase concentration decrease (ΔC_E^*) as a function of carbon dose (left panel). DOC loadings (q_{DOC}) and corresponding aqueous-phase concentration decreases (ΔC_{DOC}) as a function of carbon dose (left panel). Results shown are for SFA-10 water. Data points in the left panel were obtained from equation (2) using experimental MIB adsorption isotherm data. The lines in the left panel were obtained from equations (3)–(6) and the parameter values shown in Table 3S and 4S (supplementary information). The plots in the right panel were obtained from experimental DOC adsorption isotherm data. The lines in the right panel were obtained from corresponding Freundlich isotherm model fits.

scale in Fig. 5S (supplementary information). DOC isotherms were modeled by the Freundlich isotherm equation, as shown in Fig. 3S, and q_{DOC} values for Fig. 5S were calculated for the carbon dose, at which 50% of the initial aqueous-phase DOC concentration was adsorbed (Ando et al., 2010). The correlations in Fig. 5S are fairly strong with coefficients of determination ranging from 0.84 to 1.00. Slope values ranged from −0.27 to −0.62 (Fig. 5S), illustrating that NOM accessed a substantial fraction of the interior region of the adsorbent particles. The absolute value of the inverse of an exponent shown in Fig. 5S represents the penetration index for a given NOM. When the penetration index values were plotted against $C_{E,0}^*$ (Fig. 6), a fairly good correlation was obtained ($r^2 = 0.56$). NOM-containing waters with a high initial concentration of competing NOM (represented by $C_{E,0}^*$), such as Kasumigaura water, had a large penetration index. A large penetration index value indicates that NOM molecules can access a large fraction of the interior region of adsorbent particles. Therefore, the correlation shown in Fig. 6 suggests that NOM molecules that are able to access the interior region of adsorbent particles to a greater extent exert a greater degree of adsorption competition. Small penetration index values, on the other hand, indicate that NOM principally adsorbed close to the external particle surface and did not compete as strongly with MIB for adsorption sites. For such waters (e.g., SHA-08), $C_{E,0}^*$ and q_E^* values are small.

3.4. Characteristics of competing NOM

Prior research has shown that the low-MW NOM fraction competes directly with strongly adsorbing micropollutants (Newcombe et al., 1997, 2002b; Hepplewhite et al., 2004; Kilduff et al., 1998; Matsui et al., 2002). In this study, the fraction of NOM below a given target MW (MW_T) was estimated from HPSEC data according to equations (7) and (8):

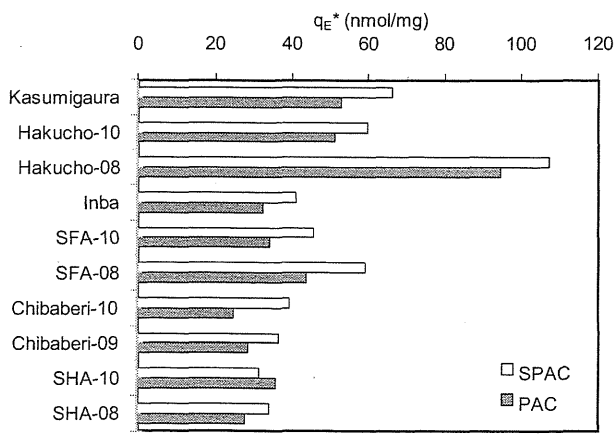

Fig. 4 – Pseudo solid-phase concentrations of the competing NOM fraction (q_E^*) at experimental conditions matching those described for Fig. 1.

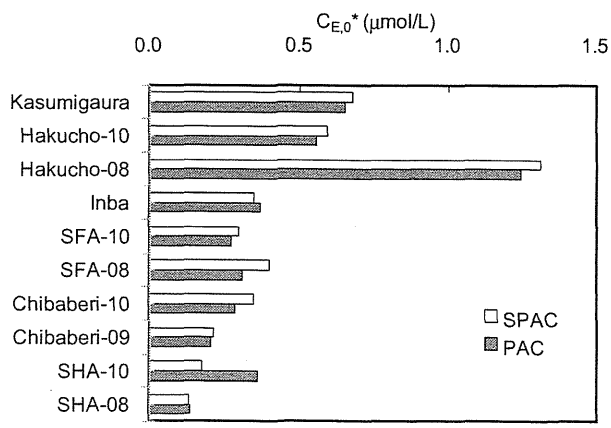

Fig. 5 – Initial pseudo aqueous-phase concentrations of competing NOM fractions ($C_{E,0}^*$) in the tested NOM-containing waters.

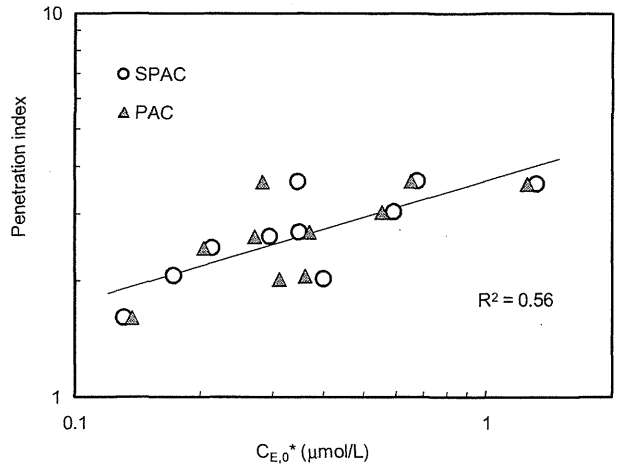

Fig. 6 – Relationship between penetration index (absolute value of gradient: log D_{50}/log q_{DOC}) and initial pseudo aqueous-phase concentration ($C_{E,0}^*$) of the competing NOM fraction.

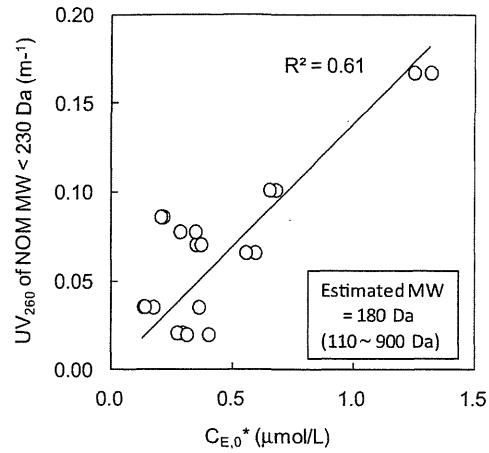

Fig. 7 – Relationship between the UV_{260} absorbance of NOM with a molecular weight smaller than 230 Da and the competing NOM concentration ($C_{E,0}^*$). UV_{260} absorbance values were obtained from size-exclusion chromatograms. $C_{E,0}^*$ values were estimated from MIB isotherms by using equations (3)–(6). Coefficients of determination (R^2) were determined from 1-SSreg/SStot, where SSreg is the sum of squares of the residuals around the regression line with an intercept of 0, and SStot is the sum of squares of the residuals around a horizontal line representing the mean absorbance value of the data shown (Motulsky and Christopoulos, 2004).

$$\text{DOC of NOM with MW} < \text{MW}_T = \text{Initial DOC} \times \text{Fraction } (<\text{MW}_T \text{ in DOC MW chromatogram}) \quad (7)$$

$$UV_{260}\text{of NOM with MW} < \text{MW}_T = \text{Initial } UV_{260} \times \text{Fraction } (<\text{MW}_T \text{ in } UV_{260}\text{MW chromatogram}) \quad (8)$$

Correlations between the NOM fraction with MW < MW_T and the initial pseudo aqueous-phase concentration of the competing-NOM ($C_{E,0}^*$) were tested by changing MW_T. As shown in Fig. 6S, a fairly good correlation ($R^2 > 0.6$) was observed for UV_{260} when MW_T was 230 Da (Panel K).

The MW of the competing NOM was further estimated by using the gradients of the regression lines in Fig. 6S. In Fig. 6S, $C_{E,0}^*$ (x-axis value) is the molar concentration of the competing NOM multiplied by $n_E^{n_M/(n_M-1)}$, and is obtained from equations (3)–(6) while y-axis values are carbon mass concentration (DOC, mg-C/L) or UV absorbance (UV_{260}, m^{-1}). Therefore,

$$\text{Gradient}\left(\text{DOC}/C_{E,0}^*\right) = \frac{\text{Carbon content} \times \text{MW}}{n_E^{\frac{n_M}{n_M-1}}} \quad (9)$$

$$\text{Gradient}\left(UV_{260}/C_{E,0}^*\right) = \frac{\text{SUVA} \times \text{Carbon content} \times \text{MW}}{n_E^{\frac{n_M}{n_M-1}}} \quad (10)$$

When SUVA (specific UV absorbance), carbon content, n_E for the competing NOM fraction, and n_M for MIB are known, the MW of the competing NOM fraction can be estimated from equations (9) and (10). Using the values shown in Table 1 and an average value for n_M (0.47, Table 3S) resulted in the MW estimates shown in each panel of Fig. 6S. For example, the correlation in Panel A was obtained by assuming that the MW of competing NOM fraction was less than 2 kDa (MW_T = 2 kDa). However, the resulting regression line indicates that the MW of the competing NOM was 10 kDa for n_E of 0.47 (6.4 kDa for n_E of 0.6 and 51 kDa for n_E of 0.2); thus, consistency was not obtained between MW_T and the MW value resulting from the slope. Consistency in MW as well as a good correlation was observed for UV_{260} when MW_T was 230 Da (Fig. 7, Panel K of Fig. 6S). The regression line indicates the MW is 180 Da for n_E of 0.47 (110 Da for n_E of 0.6 and 900 Da for n_E of 0.2). Because this MW value is close to that of MIB (168 Da), it is highly likely that the competing NOM has a similar molecular size as the targeted micropollutant. Assuming a MW of 180 Da, competing NOM concentrations were estimated from $C_{E,0}^*$ to range from 3 to 30 μg-C/L for the different NOM-containing waters. This result suggests that the competing NOM represents only 0.2–2% of entire NOM.

4. Conclusions

SPAC more effectively adsorbed NOM than PAC at a given carbon dose. However, the higher NOM loading on SPAC did not reduce the MIB adsorption capacity more, relative to organic-free water, than the lower NOM loading on PAC. By using the simplified EBC method and MW distribution data of NOM, it was estimated that the competing NOM fraction (1) contains UV-absorbing moieties, (2) has a MW <230 Da, and (3) constitutes only 0.2–2% of the entire NOM. This NOM fraction competes with MIB for adsorption sites located in the interior region of carbon particles, and its solid-phase concentration is

not a function of carbon size (SPAC/PAC). On the other hand, the higher NOM loading on SPAC relative to PAC is a result of the adsorption of non-competing NOM on sites near the external surface of the carbon particle.

Acknowledgments

This study was supported by Grant-in-Aid for Scientific Research A (21246083) and S (24226012) from the Japan Society for the Promotion of Science, by a research grant from the Ministry of Health, Labour and Welfare, and by Metawater Co., Tokyo, Japan.

Appendix A. Supplementary information

Supplementary data associated with this article can be found, in the online version, at http://dx.doi.org/10.1016/j.watres.2012.06.002.

REFERENCES

Ando, N., Matsui, Y., Kurotobi, R., Nakano, Y., Matsushita, T., Ohno, K., 2010. Comparison of natural organic matter adsorption capacities of super-powdered activated carbon and powdered activated carbon. Water Research 44 (14), 4127–4136.

Ando, N., Matsui, Y., Matsushita, T., Ohno, K., 2011. Direct observation of solid-phase adsorbate concentration profile in powdered activated carbon particle to elucidate mechanism of high adsorption capacity on super-powdered activated carbon. Water Research 45 (2), 761–767.

Crittenden, J.C., Luft, P., Hand, D.W., 1985. Prediction of multicomponent adsorption equilibria in background mixtures of unknown composition. Water Research 19 (12), 1537–1548.

Ding, L., Marinas, B.J., Schideman, L.C., Snoeyink, V.L., Li, Q., 2006. Competitive effects of natural organic matter: parametrization and verification of the three-component adsorption model COMPSORB. Environmental Science and Technology 40 (1), 350–356.

Frick, B.R., Sontheimer, H., 1983. Adsorption equilibria in multisolute mixtures of known and unknown composition. In: Suffet, I.H., McGuire, M.J. (Eds.), Treatment of Water by Granular Activated Carbon. American Chemical Society, Washington, DC, pp. 247–268.

Gillogly, T.E.T., Snoeyink, V.L., Elarde, J.R., Wilson, C.M., Royal, E.P., 1998. ^{14}C-MIB adsorption on PAC in natural water. Journal of the American Water Works Association 90 (1), 98–108.

Graham, M.R., Summers, R.S., Simpson, M.R., MacLeod, B.W., 2000. Modeling equilibrium adsorption of 2-methylisoborneol and geosmin in natural waters. Water Research 34 (8), 2291–2300.

Hepplewhite, C., Newcombe, G., Knappe, D.R.U., 2004. NOM and MIB, who wins in the competition for activated carbon adsorption sites? Water Science Technology 49 (9), 257–265.

Kilduff, J.E., Karanfil, T., Chin, Y., Weber Jr., W.J., 1996. Adsorption of natural organic polyelectrolytes by activated carbon: a size-exclusion chromatography study. Environmental Science and Technology 30 (4), 1336–1343.

Kilduff, J.E., Karanfil, T., Weber Jr., W.J., 1998. TCE adsorption by GAC preloaded with humic substances. Journal of the American Water Works Association 90, 76–89.

Kilduff, J.E., Karanfil, T., 2002. Trichloroethylene adsorption by activated carbon preloaded with humic substances: effects of solution chemistry. Water Research 36 (7), 1685–1698.

Knappe, D.R.U., 1996 Predicting the Removal of Atrazine by Powdered and Granular Activated Carbon. Doctoral thesis, University of Illinois, Urbana, IL.

Knappe, D.R.U., Matsui, Y., Snoeyink, V.L., Roche, P., Prados, M.J., Bourbigot, M.M., 1998. Predicting the capacity of powdered activated carbon for trace organic compounds in natural waters. Environmental Science and Technology 32 (11), 1694–1698.

Mackenzie, J.A., Tennant, M.F., Mazyck, D.W., 2005. Tailored GAC for the effective control of 2-methylisoborneol. Journal American Water Works Association 97 (6), 76–87.

Matsui, Y., Kamei, T., Tambo, N., Taniguchi, K., 1993. Classification of aquatic humic substances and their activated carbon absorbability. Journal of Japan Society on Water Environment 16 (7), 497–506 (in Japanese).

Matsui, Y., Yuasa, A., Li, F., 1998. Overall Adsorption isotherm of natural organic matter. Journal of Environmental Engineering 124 (11), 1099–1107.

Matsui, Y., Colas, F., Yuasa, A., 2001. Removal of synthetic organic chemical by powdered activated carbon during ultrafiltration. II: model application. Water Research 35 (2), 464–470.

Matsui, Y., Knappe, D.R.U., Iwaki, K., Ohira, H., 2002. Pesticide adsorption by granular activated carbon adsorbers-2. Effects of pesticide and natural organic matter characteristics on pesticide breakthrough curves. Environmental Science and Technology 36 (15), 3432–3438.

Matsui, Y., Fukuda, Y., Inoue, T., Matsushita, T., 2003. Effect of natural organic matter on powdered activated carbon adsorption of trace contaminants: characteristics and mechanism of competitive adsorption. Water Research 37 (18), 4413–4424.

Matsui, Y., Fukuda, Y., Murase, R., Aoki, N., Mima, S., Inoue, T., Matsushita, T., 2004. Micro-ground powdered activated carbon for effective removal of natural organic matter during water treatment. Water Science and Technology: Water Supply 4 (4), 155–163.

Matsui, Y., Murase, R., Sanogawa, T., Aoki, H., Mima, S., Inoue, T., Matsushita, T., 2005. Rapid adsorption pretreatment with submicrometre powdered activated carbon particles before microfiltration. Water Science and Technology 51 (6–7), 249–256.

Matsui, Y., Aizawa, T., Kanda, F., Nigorikawa, N., Mima, S., Kawase, Y., 2007. Adsorptive removal of geosmin by ceramic membrane filtration with super-powdered activated carbon. Journal of Water Supply: Research and Technology - AQUA 56 (6–7), 411–418.

Matsui, Y., Ando, N., Sasaki, H., Matsushita, T., Ohno, K., 2009. Branched pore kinetic model analysis of geosmin adsorption on super-powdered activated carbon. Water Research 43 (12), 3095–3103.

Matsui, Y., Nakano, Y., Ando, N., Sasaki, H., Ohno, K., Matsushita, T., 2010. Geosmin and 2-methylisoborneol adsorption on super-powdered activated carbon in the presence of natural organic matter. Water Science and Technology 62 (11), 2664–2668.

Matsui, Y., Ando, N., Yoshida, T., Kurotobi, R., Matsushita, T., Ohno, K., 2011. Modeling high adsorption capacity and kinetics of organic macromolecules on super-powdered activated carbon. Water Research 45, 1720–1728.

Motulsky, H.J., Christopoulos, A., 2004. Fitting Models to Biological Data Using Linear and Nonlinear Regression: a Practical Guide to Curve Fitting. Oxford University Press.

Najm, I.N., Snoeyink, V.L., Richard, Y., 1991. Effect of initial concentration of a SOC in natural water on its adsorption by activated carbon. Journal American Water Works Association 83 (8), 57–63.

Newcombe, G., Drikas, M., Hayes, R., 1997. Influence of characterised natural organic material on activated carbon adsorption: 2. Effect on pore volume distribution and adsorption of 2-methylisoborneol. Water Research 31 (5), 1065–1073.

Newcombe, G., Morrison, J., Hepplewhite, C., 2002a. Simultaneous adsorption of MIB and NOM onto activated carbon. I. Characterisation of the system and NOM adsorption. Carbon 40 (12), 2135–2146.

Newcombe, G., Morrison, J., Hepplewhite, C., Knappe, D.R.U., 2002b. Simultaneous adsorption of MIB and NOM onto activated carbon - II. Competitive effects. Carbon 40 (12), 2147–2156.

Nowack, K.O., Cannon, F.S., Mazyck, D.W., 2004. Enhancing activated carbon adsorption of 2-methylisoborneol: methane and steam treatments. Environmental Science and Technology 38 (1), 276–284.

Qi, S., Schideman, L., Mariñas, B.J., Snoeyink, V.L., Campos, C., 2007. Simplification of the IAST for activated carbon adsorption of trace organic compounds from natural water. Water Research 41 (2), 440–448.

Tennant, M.F., Mazyck, D.W., 2003. Steam-pyrolysis activation of wood char for superior odorant removal. Carbon 41 (12), 2195–2202.

Worch, E., 2010. Competitive adsorption of micropollutants and NOM: a comparative study of different model approaches. Journal of Water Supply: Research and Technology - AQUA 59 (5), 285–297.

Zoschke, K., Engel, C., Börnick, H., Worch, E., 2011. Adsorption of geosmin and 2-methylisoborneol onto powdered activated carbon at non-equilibrium conditions: Influence of NOM and process modeling. Water Research 45 (15), 4544–4550.

Zhou, Q., Cabaniss, S.E., Maurice, P.A., 2000. Considerations in the use of high-pressure size exclusion chromatography (HPSEC) for determining molecular weights of aquatic humic substances. Water Research 34 (14), 3505–3514.

「報　文」

水道水質試験の標準液調製における不確かさと定量精度に影響を及ぼす要因

田　原　麻衣子
国立医薬品食品衛生研究所
生活衛生化学部第三室・薬博

中　島　晋　也
熊本県立大学大学院
環境共生学研究科
西川計測株式会社

杉　本　直　樹
国立医薬品食品衛生研究所
生活衛生化学部第三室長・薬博

有　薗　幸　司
熊本県立大学大学院
環境共生学研究科・薬博

西　村　哲　治
国立医薬品食品衛生研究所
生活衛生化学部長・薬博

要旨：水道水質試験の定量分析では、試料調製から機器分析の一連の試験操作に起因して、得られる値にばらつきが生じるが、この不確かさの評価法は明確にされていない。本研究では、農薬ブタミホスの定量分析をモデル実験として、標準液調製時の不確かさを検証した。その結果、天秤、調製器具、実験者、測定機器に不確かさを生じ、0.05 mg/L の測定結果に付随する合成標準不確かさは1.63%となった。さらに、qNMR によりブタミホス市販標準品３社３製品の絶対純度を測定した結果、90.3、94.7、94.8%であり、このメーカー間差が大きな不確かさを与え、分析精度に影響を及ぼしていることが明らかとなった。

キーワード：不確かさ※、信頼性、精度管理、純度※、定量分析※
分類項目：水質管理一般（120101）、試験方法一般（120201）、試験機器・器具・試薬（120203）、精度管理（120204）、機器分析（120205）

1. はじめに

定量分析では、様々な誤差要因により、得られる値にある程度のばらつきが生じる。この測定量のばらつきを数値として具体的に表した「不確かさ」は、計測の分野で急速に広まってきた考えであり、「測定の結果に付記される、合理的に測定量に結び付けられ得る値のばらつきを特徴づけるパラメータ」と国際的に定義されている[1,2]。分析法の開発過程では、一般に併行精度を立証するバリデーションが行われるが、得られた分析値の真度と確度を評価するものではないため、一連の操作および測定の不確かさの評価が別途重要視され始めている。実際に、近年、分析結果の信頼性を示す指標の一つとして不確かさを表記することが要求されつつある。しかし、水道水質試験の場合は、定量分析値を得るまでの過程に不確かさの要因が多いため、試料および標準液の調製、機器分析における不確かさの具体的な評価法は明確にされていない。このような背景から、水道水質試験では、得られた分析結果の信頼性を確保するため、標準手順書の作成、内部精度管理や外部精度管理等の実施を要求している。また、前処理から機器分析、データ解析までの各作業段階における誤差要因の低減のために、標準品（標準物質）の入手先、標準液調製、試料採取、機器の管理等のトレーサビリティの証明を要求している。

一方、岩村らは[3]、試薬メーカー３社の市販農薬混合標準液について、ガスクロマトグラフ／質量分析計（GC/MS）により、標準液中に含まれる68種の農薬の濃度を定量し、５%の危険率で一

元配置分散分析および多重比較したところ、68物質中30物質に有意差が認められたと報告している。このように市販標準品の純度や市販標準液の濃度を評価した報告[3~6]は少ないが、市販標準品の純度および市販標準液中の物質の濃度が試薬メーカー間で異なる可能性は否定できない。すなわち、異なる試薬メーカーの市販標準品を用いて精度管理を行った場合、室内および室間精度は現実には検証できず、結果として各機関において得られた定量値の信頼性が厳密な意味で確保できないこともあり得ると考えられる。

そこで本研究では、水道水質試験における標準液調製時に生じる不確かさを評価し、定量精度の信頼性を確保するための要因を明らかとする目的で、水環境中で検出される恐れのある農薬として水質管理目標設定項目にも挙げられているブタミホスを測定対象としたモデル実験を行った。

2. 装置および調査方法等

2.1 標準品および試薬

ブタミホス市販標準品として、市販残留農薬試験用標準品3社3製品A（林純薬工業株式会社、Cat. No. 990-52021、Lot J091016037、純度99.9％（GC/FID））、B（和光純薬工業株式会社、Cat. No. 020-10931、Lot ALK8029、純度99.8％（GC/FID））、C（関東化学株式会社、Cat. No. 04346-96、Lot 708X7110、純度99.2％（GC/FID））を用いた。フタル酸ジエチル（diethyl phthalate: DEP）は独立行政法人産業技術総合研究所の認証標準物質（NMIJ CRM 4022-b、純度99.98±0.01 w/w％（99.74±0.09 mol/mol％））を用いた。高純度ヘキサメチルジシラン（hexadimethyldisilane: HMD）は和光純薬工業株式会社特注品、重メタノールはIsotec（99.8 atom％ D）を用いた。アセトンおよびアセトニトリルは高速液体クロマトグラフ用（和光純薬工業株式会社）、ギ酸は試薬特級（和光純薬工業株式会社）を用いた。精製水はElix純水装置システム（日本ミリポア株式会社）より得たものを用いた。

2.2 試料調製に用いた器具および機器

20 mLメスフラスコ（IWAKI PYREX、許容誤差0.04 mL（20℃））、100 μLマイクロシリンジ（HAMILTON SYRINGE 80665、Lot 279510、許容誤差1％以内）、2.0 mLメスピペット（PYREX pipet 7077-2N、disposable glass、serological、individual wrap、sterile、7740 glass、許容誤差1％以内）を試料調製に用いた。

天秤は、ウルトラミクロ天秤XP2U（メトラー・トレド株式会社、最小計量値0.6 mg）およびセミミクロ天秤R200D（ザルトリウス・メカトロニクス・ジャパン株式会社、最小計量値4.8 mg）を用いた。なお、各天秤の最小計量値は、USP-NF Weights and Balances[7]に準じ、実測値より計算した。

液体クロマトグラフ／フォトダイオードアレイ検出器（LC/PDA）は、Acquity UPLC/PDA（日本ウォーターズ株式会社）を用いた。

核磁気共鳴装置（NMR）は、オートサンプラー付きJNM-ECA600（日本電子株式会社、600 MHz）を用いた。

2.3 試料調製および不確かさの評価

ブタミホス標準原液は、市販標準品製品A 20 mgを精密に量り取り、メスフラスコで20 mLに定容して1,000 mg/Lのアセトン溶液とし（図-1 段階1）、－20℃で保存したものを用いた。0.05、0.5、5 mg/Lの標準液は、ブタミホス標準原液をアセトンで希釈し、用時調製した。すなわち、5 mg/L標準液は1,000 mg/L標準原液をマイクロシリンジで100 μLとり、メスフラスコで20 mLに定容した（段階2）。また、0.5 mg/L標準液は5 mg/L標準液からメスピペットで2.0 mLとり20 mLに定容し（段階3）、同様に0.5 mg/L標準液からメスピペットで2.0 mLとり20 mLに定容し、0.05 mg/L標準液とした（段階4）。

実験者の調製の不確かさは、アナログ計器の読み取りの偏りとして求めた。希釈に用いたメスフラスコ、メスピペットおよびマイクロシリンジについて、精製水を正確に量り取り、その重量を秤量し、25回試行において得られた実験標準偏差（SD）により相対標準偏差（RSD）を算出した。また、調製した標準液を液体クロマトグラフ／フォトダイオードアレイ検出器（LC/PDA）に付し、クロマトグラム上に観察されたブタミホスのピーク面積値について、25回測定におけるRSDを算出し、繰り返し測定における不確かさとした。な

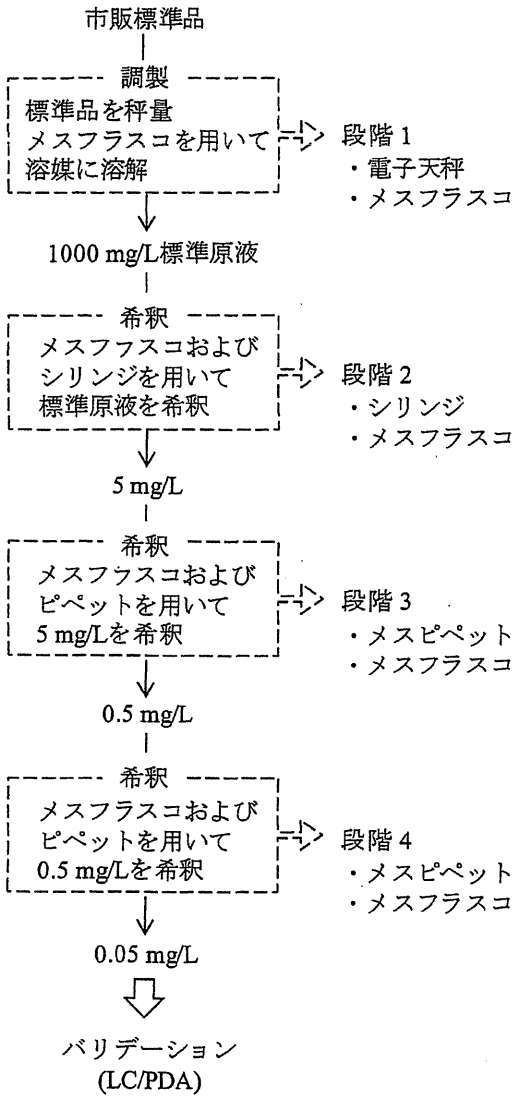

図-1　標準液調製の過程と使用機器および器具
調製過程は段階1-4に分類し、各段階で使用した機器および器具を示した。

お、本研究の実験は通常の試験を想定して室温で行い、秤量時の重力や温度のような測定環境の変動に関する不確かさ[8]は考慮しないこととした。

2.4　機器分析条件

LC/PDA による分析の測定条件は、カラム、Discovery HS F5 (150×2.1 mm、5 μm、SUPELCO)；カラム温度、40℃；移動相は0.1%ギ酸：アセトニトリル＝20：80；流量、0.2 mL/min；注入量、10 μL；検出波長、260 nm で行った。すべての測定は1試料につき25回測定し、保持時間2.15分に観察されるピーク面積（0.05 mg/L の S/N 比 >200）を計測した。

ブタミホス標準品3社3製品（A、B、C）の絶対純度は、既報の定量 NMR（quantitative NMR：qNMR）[9,10]により、計量学的に正確に決定した。qNMR のケミカルシフト値は、HMD を基準シグナル（0 ppm）とし、δ値を ppm 単位で表した。データ解析は、得られた Free Induction Decay（FID）信号データを定量解析ソフトウェア（ALICE2 for qNMR、日本電子株式会社）に導入して自動処理した。このソフトウェア上では、qNMR データをフーリエ変換および自動位相調整を行い、HMD および特定シグナルの積分範囲等を設定後、HMD およびブタミホスの濃度、分子量、特定基のプロトン数等の化合物情報から、絶対純度（w/w%）を算出した。

3.　結果および考察

3.1　標準液調製における不確かさ要因の摘出

機器分析に供する標準液の調製には、通常、市販標準品製品あるいは標準原液製品を用い、分析に適した溶媒により希釈する方法を用いる。この標準液の調製過程において、標準原液の作製から希釈操作の各段階で不確かさが生じることとなる。また同様に、前処理を含めた試料調製においても各段階で不確かさが生じる。したがって、定量分析値には標準液調製、試料調製の両者の不確かさが含まれる。

モデル実験には、いわゆる微量分析のひとつである水道水検査を想定して、小容量のガラス器具を用いることとし、標準品から標準液0.05、0.5、5 mg/L を調製する各段階では、電子天秤やメスフラスコ、マイクロシリンジ、ピペットの調製器具を使用した（図-1）。これらの使用により、定量分析値に影響を及ぼす主な不確かさの要因は、図-2にフィッシュボーンダイアグラムとして示した測定器具の精度や実験者の器具の使用熟練度が考えられた。

次に、標準液調製における不確かさを求め、不確かさを大きくする主要因を検討した。不確かさには、一連の測定値の統計的解析によって評価されるAタイプと校正証明書等に記載されているBタイプがある。図-2のうち、実験者の熟練度や機器の繰り返し測定の不確かさはAタイプ、測定機器の成績評価の不確かさや器具の許容誤差は

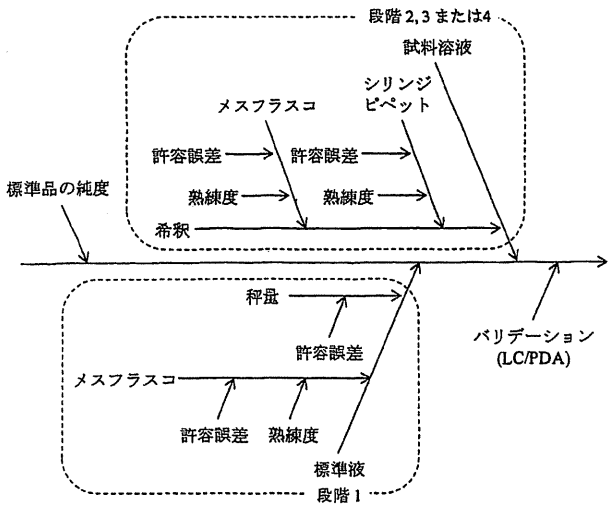

図-2　試料調製に係る不確かさの要因のフィッシュボーンダイアグラム
段階については図-1に示した。

Bタイプに分類できる。Aタイプである実験者の熟練度の不確かさについては、実験から得られた測定量の規格容量に対するばらつきを用いた。すなわち、希釈に用いたガラス容量器のメスフラスコ、マイクロシリンジおよびメスピペットは、25回試行の不確かさを算出し、それぞれ0.04240、0.3208、0.7933%となった。また、Bタイプである秤量に用いた電子天秤の拡張不確かさは、成績評価より100 mg±0.0026 mg（包含係数k=2）であった。電子天秤の不確かさは正規分布とみなし、包含係数k=2の場合は95%信頼水準に相当する。拡張不確かさは合成標準不確かさに包含係数を乗じた値であるので、電子天秤の不確かさは拡張不確かさを包含係数で除した値0.0026/2=0.0013 mg（0.0013%）とした。ガラス容量器については、JIS規格により、器具自体が持つ誤差として許容誤差が表示されている。調製器具の不確かさは、矩形分布を仮定して$\sqrt{3}$で除した値を標準不確かさとすることができる[11]。よって、希釈に用いた20 mLメスフラスコの許容誤差は±0.04 mLであったので、メスフラスコの許容誤差の不確かさは$0.04/\sqrt{3}=0.02309$ mL（0.1155%）と算出した。さらに、メスピペットおよびマイクロシリンジの許容誤差は、±1%以内であったので、ともに0.5774%と算出した。得られたすべての数値を表-1に示した。また、Aタイプであ

表-1　標準液調製における不確かさが生じる要因および測定結果に付随する不確かさ

段階	要因		タイプ[a]		不確かさ (%)	合成標準不確かさ[b] (%)	
1	電子天秤	許容誤差	B	u_1	0.0013		
	20 mL メスフラスコ	許容誤差	B	u_2	0.1155		
		熟練度	A	u_3	0.04240		
2	100 μL シリンジ	許容誤差	B	u_4	0.5774	5 mg/L	
		熟練度	A	u_5	0.3208		
	20 mL メスフラスコ	許容誤差	B	u_2	0.1155	(段階1-2)	
		熟練度	A	u_3	0.04240	0.742	
3	2.0 mL メスピペット	許容誤差	B	u_6	0.5774		0.5 mg/L
		熟練度	A	u_7	0.7933		
	20 mL メスフラスコ	許容誤差	B	u_2	0.1155	(段階1-3)	
		熟練度	A	u_3	0.04240	1.24	
4	2.0 mL メスピペット	許容誤差	B	u_6	0.5774		0.05 mg/L
		熟練度	A	u_7	0.7933		
	20 mL メスフラスコ	許容誤差	B	u_2	0.1155	(段階1-4)	
		熟練度	A	u_3	0.04240	1.63	

[a] Aタイプの不確かさは、精製水を正確に量り取って25回試行の秤量値より算出した。
Bタイプは校正証明書等に記載されている値を用いた。

[b] 0.05、0.5、5 mg/LにおけるLC/PDAによる繰り返し測定の不確かさはそれぞれ0.4762、0.2970、0.2896%であるので、合成標準不確かさは式(1)より

5 mg/L：$u_5=\sqrt{(u_1^2+u_2^2\times2+u_3^2\times2+u_4^2+u_5^2+0.2896^2)}=0.742(\%)$

0.5 mg/L：$u_{0.5}=\sqrt{(u_1^2+u_2^2\times3+u_3^2\times3+u_4^2+u_5^2+u_6^2+u_7^2+0.2970^2)}=1.24(\%)$

0.05 mg/L：$u_{0.05}=\sqrt{(u_1^2+u_2^2\times4+u_3^2\times4+u_4^2+u_5^2+u_6^2\times2+u_7^2\times2+0.4762^2)}=1.63(\%)$

るLC/PDAによる繰り返し測定の不確かさは、クロマトグラム上に観察されたブタミホスのピーク面積値について、25回測定におけるRSDを算出した。すなわち、0.05、0.5、5 mg/Lにおいてそれぞれ0.4762、0.2970、0.2896%となった。これらの結果より、不確かさは使用器具および実験者によって異なるが、相対的に大小があり、今回のモデル実験の場合、メスピペットの操作熟練度＞メスピペットおよびシリンジの許容誤差＞LC/PDA繰り返し精度＞シリンジの操作熟練度＞メスフラスコの許容誤差＞メスフラスコの操作熟練度〉〉〉電子天秤の許容誤差となった。

3.2　定量値に付随する一連の不確かさ

最終的に得られる測定量の不確かさは、調製から測定までのさまざまな不確かさ成分の合成であり、測定量に付随する推定標準偏差は合成標準不確かさで算出され、合理的に測定量に結び付けられ得る値の分散を特徴づける。このため、合成標準不確かさは不確かさの伝播則により、合成分散の正の平方根で与えられる。

測定結果yの合成標準不確かさ$u_c(y)$は

$$u_c(y)=\sqrt{(u_1^2+u_2^2+\cdots\cdots+u_n^2)} \quad \cdots\cdots\cdots\cdots\cdots\cdots(1)$$

u_1, u_2, u_n：各成分の不確かさ

であることから、ブタミホス0.05、0.5、5 mg/Lの測定結果に付随する不確かさ（u）は、表-1に示した各要因の合成で、それぞれ1.63、1.24、0.742%となり、希釈段階が増えるほど不確かさは大きくなった。95%信頼水準に相当する拡張不確かさは合成標準不確かさに包含係数を乗じた値であるので、上記の値（u）に包括係数k＝2を乗じて3.25、2.48、1.48%となった。この不確かさは、標準液測定の手順において合理的に算出されたものである。よって、水道水質試験においては、抽出や濃縮等の水試料の前処理を必要とする場合、その操作の各段階で生じる不確かさを勘案するため、測定結果に付随する不確かさはさらに大きくなると推定される。

合成標準不確かさの計算より、不確かさの小さい電子天秤の許容誤差に関しては、全体の不確かさから考えると、無視しても問題がない程度であった。一方、今回のモデル実験の場合、調製のピペットの読み取り等実験者の熟練度が全体のばらつきに影響することが推察された。精度の高い定量分析値を得るためには、水道水質試験従事者が不確かさの概念や大小を把握し、実験者の熟練度を向上、また、各段階の不確かさを可能な限り小さくするための使用器具の選定や作業手順の設定等が重要であると考えられる。また、分析操作の各段階での不確かさの算出は、分析の精度検証にも有用であることが分かった。

3.3　ブタミホス市販標準品のメーカー間の絶対純度の比較

岩村らは、市販農薬混合標準液の濃度相互比較[3]において、農薬の濃度にメーカー間の大きな有意差があることを報告しているが、標準液中に含まれる農薬の絶対量が正しいかどうかについては論じてはいない。そこで、付帯情報として、純度（GC/FIDによる主ピークの全ピーク面積に対する百分率による表示値）がそれぞれ99.9%、99.8%、99.2%と表示されたブタミホス市販標準品3社3製品（A、B、C）について、既報[9,10]の定量NMRに従い、国際単位系（SI）にトレーサブルな絶対純度を決定した。図-3にブタミホス市販標準品AのqNMRスペクトルを示す。3製品すべてにおいて、交換性のNH基由来のピークを除いたシグナル（a～j）が観察された。高磁場領域（0.5～4.5 ppm）のシグナルには不純物由来のシグナルが重なる可能性が高いため、絶対純度の決定には低磁場領域のシグナルを用いることとし、芳香族性プロトンであるh、i、jの3つシグ

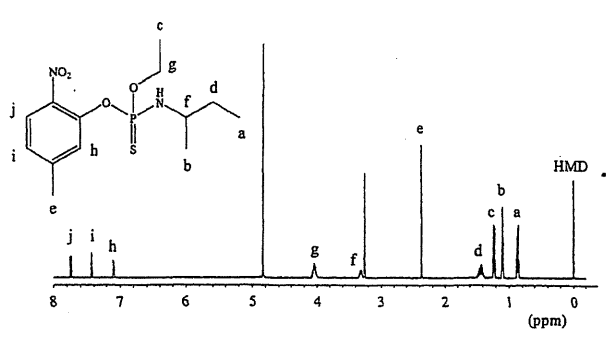

図-3　ブタミホス市販標準品AのNMRスペクトル
HMDをqNMRの内標準物質および基準シグナル（δ0 ppm）として使用した。ブタミホスのプロトンの帰属をスペクトルおよび構造式上にアルファベットで示した。

ナルを利用した。ブタミホス市販標準品3社3製品（A、B、C）のブタミホスの絶対純度を求めた結果、それぞれの絶対純度（RSD%、n=3）は、94.8（0.7）%、94.7（0.8）%、90.3（0.6）%であった（表-2）。

以上のことから、ブタミホス標準品製品の添付文書に記載された表示値と絶対純度値の間に5.1～8.9%の差異が存在し、標準品製品の表示値は絶対量（絶対純度）を示していないことが明らかとなった。

3.4　異なった市販標準品を用いた場合に生じる定量値の不確かさ

添付文書に記載された表示値の純度により定量値を算出した場合、標準品3製品の表示値がほぼ100%であるため、試験法通りに実施することによって分析値は見かけ上精度が取れている。しかし、3.3項で示したように、多くの市販標準品製品の表示値は、標準品製品中の主成分の相対量を示すものであり、絶対量（絶対純度）を示したものではない。よって、市販標準品製品間の絶対純度のばらつきは得られる定量値の不確かさ要因となる。そこで、3社間の絶対純度のばらつきと調製過程を含めて、標準品から測定までの一連の操作から得られた定量値の不確かさを試算した。

添付文書に記載された表示値を純度とし、定量値を100%と換算すると、qNMRにより算出されたブタミホス市販標準品3社3製品A、B、Cの絶対純度における定量値の割合はそれぞれ94.9、94.9、91.0%となることから、これらのメーカー間の不確かさ（RSD）は2.23%と求められる。次に、ブタミホス標準液0.05 mg/Lの操作過程における不確かさ（3.2項より1.63%）に、メーカー間の不確かさおよびqNMR測定の不確かさ（A、B、Cそれぞれ0.716、0.839、0.555%）を考慮したブタミホス標準液0.05 mg/Lの測定結果に付随する合成標準不確かさは、

$$u_{qNMR} = \sqrt{(2.23^3+0.716^2+0.839^2+0.555^2+1.63^2)} = 3.03(\%)$$

となり、拡張不確かさは6.05%（k=2）となった。

したがって、絶対純度が保証されていない市販標準品製品を定量用標準物質として定量分析に用いた場合、メーカー間の絶対純度のばらつきが、最終的に得られる定量値に大きな不確かさを与える主要因となり得ることが示唆された。

表-2　ブタミホスの市販標準品3社3製品のqNMRによる絶対純度と添付文書の純度値との比較

qNMRによる純度（%）	ブタミホス市販標準品 A	B	C	3製品の平均±RSD（%）
シグナル（ppm）				
h 7.09	94.5	94.4	90.1	
i 7.42	94.9	95.0	90.4	
j 7.74	94.9	94.7	90.5	
シグナル平均（%）	94.8	94.7	90.3	93.3±2.57
シグナル間RSD（%）	0.2	0.3	0.2	
添付文書で示されたGC/FIDによる純度値（%）	99.9	99.8	99.2	99.6±0.379

4.　まとめ

本研究では、水道水質試験の微量分析を想定した標準液調製のモデル実験を行い、各段階において不確かさが生じる要因を検証した。その結果、標準液調製の一連の中で、不確かさは電子天秤、調製器具、実験者、機器分析のすべての過程に生じた。使用する調製器具によって大小はあるが、器具操作の熟練度＞器具の許容誤差＞LC/PDA繰り返し精度＞電子天秤の許容誤差という傾向が観察され、今回のモデル実験の場合、メスピペットの操作熟練度が大きな要因となることが明らかとなった。また、定量NMRによる市販標準品3社3製品の絶対純度測定を行った結果、メーカー表示の純度値が絶対値を示していないことが明らかとなった。さらに、市販標準品製品の絶対純度にはメーカー間差が存在することを証明すると共に、このメーカー間差が定量分析値の不確かさを大きくする要因となり、その精度に影響を与えていることが示唆された。

以上のことから、定量値の精度および確度を向上させるためには、分析技術者自身の技術レベルの向上だけでなく、絶対純度が明確な標準物質の供給と入手が、重要なファクターであることが明らかとなった。実際の分析および検査の過程には、今回の標準液の調製以外にも試料の前処理や調製過程が含まれるため、分析値の信頼性確保にはさらに各段階の不確かさの検証が必要であると考えられる。さらに、機器分析において、試料の注入